IEICE TRANS. INF. & SYST., VOL.E84–D, NO.3 MARCH 2001

PAPER

Firing Patterns Depending on Model Neurons

Kazushi MURAKOSHI[†] *and* **Kiyohiko NAKAMURA**[†], *Regular Members*

SUMMARY An electrophysiological experiment showed that spike timing was precise to less than one millisecond. This result indicates the possibility in the precise time codings. For a high accurate time coding, reconsideration of a neural mechanism which decides firing time is required. From such viewpoint, we quantitatively examined change in firing time with interference between two synaptic inputs through Hodgkin-Huxley (HH) and integrate-and-fire (IF) model neurons. The precise firing times in the HH model neuron were extremely different from those in the IF model neuron. In this paper, the relations of input intensity to firing time are investigated in the other more two pulse generation models: Morris-Lecar (ML) and FitzHugh-Nagumo (FN) model. The result of the ML model in a certain parameter set (type-I) exhibited monotone decreasing like that of the IF model while the result of the ML model in the otter parameter set (type-II) exhibited non-monotone decreasing like that of the HH model. The result of the FN model exhibited non-monotone decreasing like the HH model despite its qualitativeness. Next the firing patterns in the four model neurons on a model of V1 (primary visual area) and LGN (lateral geniculate nucleus) with circular and mutual excitatory connections are investigated to show how dependent on model neurons the firing patterns are. The spikes in the HH, the ML type-II, and the FN model neurons elicited synchronous oscillations while the spikes in the IF and the ML type-I model neurons did not; the firing patterns dramatically changed with the dependence on the model neurons.

key words: *Hodgkin-Huxley model, integrate-and-fire model, Morris-Lecar model, FitzHugh-Nagumo model, oscillatory synchrony*

1. Introduction

An electrophysiological experiment showed that spike timing was precise to less than one millisecond [1]. This result indicates the possibility in the precise time codings. It is expected that the information processing ability is improved in comparison with average firing rate coding, if the spike time coding is possible [2]. For a high accurate time coding, reconsideration of a neural mechanism which decides firing time is required.

One of the simplest spike time coding would be spiking time from the beginning of input time. The relation of the intensity of single input to the firing time is monotone decreasing: a strong input generates a spike faster than a weak one does [3]–[5]. This relation will hold even when the input is from multiple spikes, as long as the spikes are almost simultaneous. In actuality, however, numerous synaptic inputs arriving at various times are gathered into a single neuron. In such a situation it is not easy to forecast firing time.

From such a viewpoint, we quantitatively examined change in firing time with interference between two synaptic inputs through Hodgkin-Huxley (HH) and integrate-and-fire (IF) model neurons [6]. The precise firing times in the HH model neuron were extremely different from those in the IF model neuron.

This paper aims to elucidate precise firing patterns of model neurons furthermore. First this paper investigates firing times by interference between two synaptic inputs through the two more well-studied spiking neuron models: Morris-Lecar (ML) and FitzHugh-Nagumo (FN) model neurons. The ML model is formulated to describe a variety of oscillation while the FN model is derived by reducing the parameter of the HH model.

In our previous work, the precise firing times in the HH model neuron was extremely different from those in the IF model. It is expected that the firing patterns of neural circuits in the HH like model also differs those in the IF like model. Second the firing patterns in the four model neurons in an example of a connective model is investigated to show how dependent on model neurons the firing patterns are.

2. Firing Time by Interference between Spikes

In four model neurons, we investigate the firing time by interference between two synaptic inputs: fixed base input and control input which is varied with intensity and relative input time from the beginning of the base input. Here firing time is defined as the time from the beginning of the base input to the time the membrane potential V exceeds the threshold.

Our previous work showed that firing time is not a monotonically decreasing function of the previous input intensity of two successive input especially in weak positive input one in the HH model [6]. In this paper, therefore, we use excitatory input only.

All differential equations were solved with a fourth-order Runge-Kutta method with a time step of 0.001 ms. The base input in each model neuron is taken from near the center of the curve of firing time by single synaptic input to investigate property of firing in each model neuron.

Manuscript received September 30, 1999.
Manuscript revised August 21, 2000.

[†]The authors are with the Department of Computational Intelligence and Systems Science, Interdisciplinary Graduate School of Science and Engineering, Tokyo Institute of Technology, Yokohama-shi, 226–8502 Japan.

Table 1 Hodgkin-Huxley variables and parameters used in the simulations [7].

$I_{ext}(t)$	:	external current density [μA/cm^2] (outward current positive)
V	:	membrane potential [mV]
m	:	sodium activation ($0 < m < 1$) initial value $m_0 = 0.042$
h	:	sodium inactivation ($0 < h < 1$) initial value $h_0 = 0.608$
n	:	potassium activation ($0 < n < 1$) initial value $n_0 = 0.315$
t	:	time [ms]
C_m	:	membrane capacity per unit area [1 μF/cm^2]
$\bar{g}_{Na}$	:	maximal sodium conductance [120 mS/cm^2]
$\bar{g}_K$	:	maximal potassium conductance [36.0 mS/cm^2]
$\bar{g}_l$	:	maximal leak conductance [0.3 mS/cm^2]
V_{Na}	:	equilibrium sodium potential [55.0 mV]
V_K	:	equilibrium potassium potential [-72.0 mV]
V_l	:	equilibrium leak potential [-49.387 mV]
Θ	:	temperature [15 °C]
ϕ	:	temperature-scaling factor
$\alpha,\ \beta$	:	rate constant [ms^{-1}]
α_m	=	$\frac{0.1(-35.0-V)}{\exp\left(\frac{-35.0-V}{10.0}\right)-1.0}$ ($\alpha_m = 1.0$ if $V = -35.0$)
β_m	=	$4.0\exp\left(-\frac{60.0+V}{18.0}\right)$
α_h	=	$0.07\exp\left(-\frac{60.0+V}{20.0}\right)$
β_h	=	$\frac{1.0}{\exp\left(\frac{-30.0-V}{10.0}\right)+1.0}$
α_n	=	$\frac{0.01(-50.0-V)}{\exp\left(\frac{-50.0-V}{10.0}\right)-1.0}$ ($\alpha_n = 0.1$ if $V = -50.0$)
β_n	=	$0.125\exp\left(-\frac{60.0+V}{80.0}\right)$
ϕ	=	$3.0^{\frac{(\Theta-6.3)}{10.0}}$

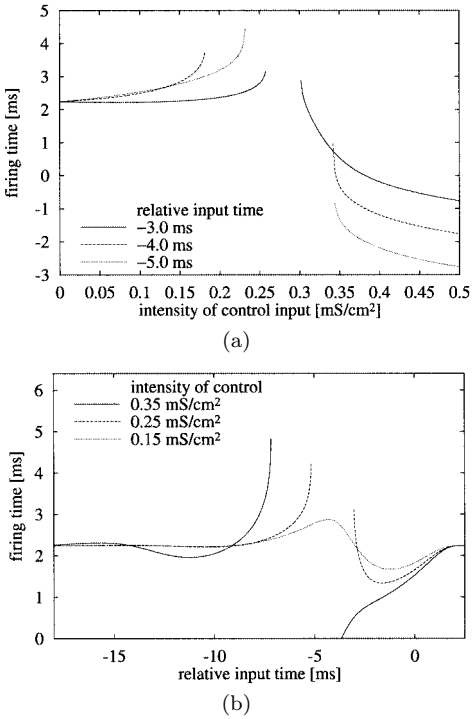

Fig. 1 Relations between input and firing time. (a) Relation of input intensity to firing time by interference between two inputs. The base input intensity is 0.5 mS/cm^2. (b) Relation of relative input time to firing time by interference between two inputs. At 0.35 mS/cm^2 input intensity, the neuron also fires before time zero when the relative time is less than -3 ms. The reason why the curves are interrupted is that neuron cannot fire for interference by previous synaptic input or that neuron previously fires by the control input.

2.1 Hodgkin-Huxley Model

Hodgkin-Huxley model [7] consists of four differential equations:

$$\frac{dV}{dt} = \frac{1}{C_m}\left[I_{ext}(t) - \bar{g}_{Na}m^3h(V - V_{Na}) - \bar{g}_K n^4(V - V_K) - \bar{g}_l(V - V_l)\right], \quad (1)$$

$$\frac{dm}{dt} = \phi\left[\alpha_m(1 - m) - \beta_m m\right], \quad (2)$$

$$\frac{dh}{dt} = \phi\left[\alpha_h(1 - h) - \beta_h h\right], \quad (3)$$

$$\frac{dn}{dt} = \phi\left[\alpha_n(1 - n) - \beta_n n\right]. \quad (4)$$

The variables and parameters are listed in Table 1.

An external current stimulus $I_{ext}(t)$ is expressed by a time-varying synaptic conductance $g_{\rm syn}(t)$[mS/cm^2], which is represented by an α function [8], [9]:

$$g_{{\rm syn}i}(t) = \begin{cases} A_i\frac{t-t_i^f}{\tau_i^2}\exp(-\frac{t-t_i^f}{\tau_i}) & \text{if} \quad t \geq t_i^f \\ 0 & \text{if} \quad t < t_i^f \end{cases}, \quad (5)$$

$$I_{ext}(t) = -\sum_i g_{{\rm syn}i}(t)(V - V_{\rm rev}) \quad (6)$$

where t_i^f is the arrival time of i-th spike and τ_i is the time giving the maximum conductance A_i. We simply set all $\tau_i = 1.5$ ms as time course of AMPA excitatory receptor. $V_{\rm rev}$ is the reversal potential: $V_{\rm rev} = 0$ mV for an excitatory input. The neuron fires when its membrane potential V exceeds the threshold, -45 mV.

The results are shown in Figs. 1 (a) and (b). Figure 1 (a) shows firing time as a function of control input intensity for several discrete relative input times. It is noteworthy that the firing time is lengthened despite excitatory control input when the relative input time is a certain negative.

Figure 1 (b) shows firing time for relative input time in several discrete intensities of control input. These results indicate that firing time can be longer or shorter depending on relative input time between two inputs of fixed intensity by interference between them.

2.2 Integrate-and-Fire Model

The differential equation for membrane potential V in integrate-and-fire model [10] is

$$\tau_m\frac{dV}{dt} = r_m I_{ext}(t) - V + V_0. \quad (7)$$

The variables and parameters are listed in Table 2.

Table 2 Integrate-and-fire variables used in the simulations.

$I_{ext}(t)$	:	external current density [μA/cm^2]
r_m	:	membrane surface resistance [1 kΩcm^2]
V	:	membrane potential [mV]
		resting potential $V_0 = -60$
t	:	time [ms]
τ_m	:	membrane time constant [5 ms]

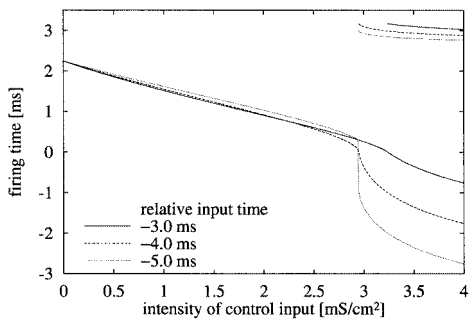

(a)

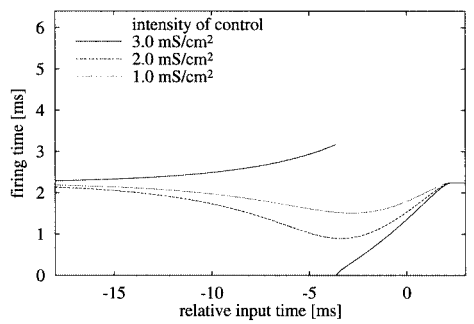

(b)

Fig. 2 Relations between input and firing time in the case of the integrate-and-fire model. (a) Relation of input intensity to firing time by interference between two inputs. The base input intensity 4.0 mS/cm^2. (b) Relation of relative input time to firing time by interference between two inputs. At 3.0 mS/cm^2 input intensity, the neuron also fires before time zero when relative time is less than -3 ms.

The neuron fires when its membrane potential exceeds the threshold (-45 mV), and the membrane potential decreases (-70 mV) after firing. The external input current $I_{ext}(t)$ is the same one given by Eq. (5) in the HH model.

Figure 2 (a) shows the relation of control input intensity to firing time for some fixed relative input times. All relations are monotone decreasing. These results differ from the results obtained using the HH model. Figure 2 (b) shows the relation of relative input time to firing time for some fixed control input intensities. Unlike what was seen with the HH model, the firing times for the positive control input are always shortened. When the intensity is 3.0 mS/cm^2, however, the firing time is long because of the decrease to -70 mV after the previous firing.

Table 3 Morris-Lecar variables used in the simulations [11], [13].

$I_{ext}(t)$	:	external current density [μA/cm^2]
V	:	membrane potential [mV]
N	:	fraction of open potassium channels ($0 < N < 1$)
t	:	time [ms]
C_m	:	membrane capacity per unit area [μF/cm^2]
$\bar{g}_{Ca}$	:	maximal calcium conductance [mS/cm^2]
$\bar{g}_K$	:	maximal potassium conductance [mS/cm^2]
$\bar{g}_l$	:	maximal leak conductance [mS/cm^2]
V_{Ca}	:	equilibrium calcium potential [mV]
V_K	:	equilibrium potassium potential [mV]
V_l	:	equilibrium leak potential [mV]
V_1	:	potential at which $N_\infty = 0.5$ mV
V_2	:	reciprocal of slope of M_∞
V_3	:	potential at which $N_\infty = 0.5$ mV
V_4	:	reciprocal of slope of N_∞
$M_\infty(V)$	=	$0.5(1 + \tanh((V - V_1)/V_2))$
$N_\infty(V)$	=	$0.5(1 + \tanh((V - V_3)/V_4))$
τ_N	=	$\frac{1}{\phi_N \cosh((V-V_3)/2V_4))}$

Table 4 Morris-Lecar parameters used in the simulations [11], [13].

Variable	type-I	type-II
C_m [μF/cm^2]	5.0	5.0
$\bar{g}_{Ca}$ [mS/cm^2]	4.0	4.4
$\bar{g}_K$ [mS/cm^2]	8.0	8.0
$\bar{g}_L$ [mS/cm^2]	2.0	2.0
V_{Ca} [mV]	120.0	120.0
V_K [mV]	-84.0	-84.0
V_L [mV]	-60.0	-60.0
V_1 [mV]	-1.2	-1.2
V_2 [mV]	18.0	18.0
V_3 [mV]	12.0	0.0
V_4 [mV]	17.4	36.0
ϕ_N	0.8	0.6

2.3 Morris-Lecar Model

Morris et al. [11] formulated a model intended to explain the varied oscillatory and bistable behavior seen in experiments with barnacle muscle fiber. The Morris-Lecar (ML) model is utilized for a single neuronal oscillatory phenomenon [11]–[13]. The ML model is expressed by following three differential equations:

$$\frac{dV}{dt} = \frac{1}{C_m}\left[I_{ext}(t) - \bar{g}_{Ca}M_\infty(V)(V - V_{Ca}) - \bar{g}_K N(V - V_K) - \bar{g}_L(V - V_L)\right], \quad (8)$$

$$\frac{dN}{dt} = \frac{N_\infty(V) - N}{\tau_N}. \quad (9)$$

The variables and parameters of the modified ML models (type-I and type-II) [12], [13] are listed in Tables 3 and 4. The classification was proposed by Hodgkin [3], who found arbitrarily low response frequencies and spike latencies (type-I) and a narrow range of responses with no spike delay (type-II). The neuron fires when its membrane potential exceeds the threshold (-12 mV). The external input current $I_{ext}(t)$ is the same one given

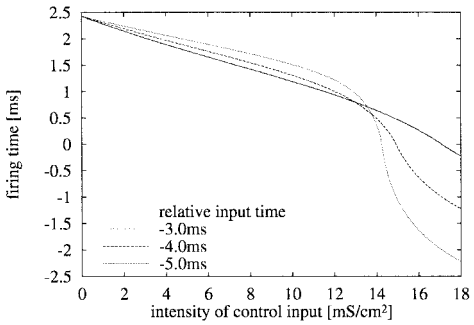

(a)

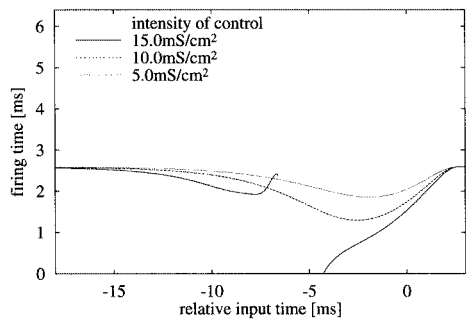

(b)

Fig. 3 Relation of input intensity to firing time by interference in the case of the Morris-Lecar type-I model. (a) Relation of input intensity to firing time by interference between two inputs. The base input intensity is 18.0 mS/cm^2. (b) Relation of relative input time to firing time by interference between two inputs. At 15.0 mS/cm^2 input intensity, the neuron also fires before time zero when relative time is less than −4 ms.

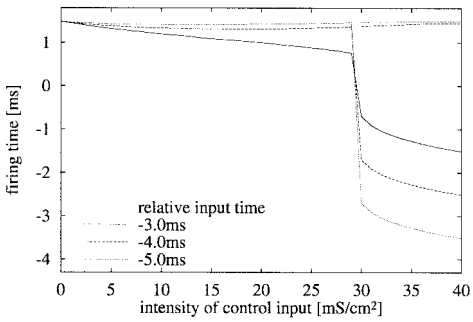

(a)

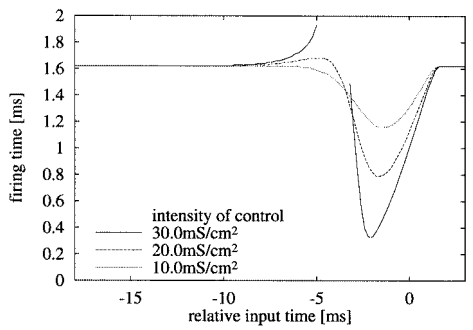

(b)

Fig. 4 Relation of input intensity to firing time by interference in the case of the Morris-Lecar type-II model. (a) Relation of input intensity to firing time by interference between two inputs. The base input intensity 40.0 mS/cm^2. (b) Relation of relative input time to firing time by interference between two inputs.

by Eq. (5) in the HH model.

Figures 3 (a) and 4 (a) shows the results of the relations of control input intensity to firing time for the ML type-I and type-II model, respectively. The relations of the control input intensity to the firing time for the type-II model are not monotone decreasing while the relations for the type-I model are monotone decreasing.

2.4 FitzHugh-Nagumo Model

FitzHugh-Nagumo (FN) model is derived by reducing the parameter the HH model. FitzHugh [14], [15] and, independently, Nagumo, Arimoto, and Yoshizawa [16] derived the following two equations to qualitatively describe the events occurring in an neuron:

$$\frac{dV}{dt} = V - \frac{V^3}{3} - W + I_{ext}(t) \tag{10}$$

$$\frac{dW}{dt} = \phi(V + a - bW) \tag{11}$$

The variables and parameters are listed in Table 5. The resting potential is −1.2, so the reversal potential $V_{\rm rev}$ and threshold value are scaled down: $V_{\rm rev} = 0$ for an excitatory input and threshold value is −0.9.

Figure 5 shows the results of relations of control input intensity to firing time. All relations are not monotone decreasing.

Table 5 FitzHugh-Nagumo variables used in the simulations.

$I_{ext}(t)$	:	external current
V	:	membrane potential resting potential $V_0 = -1.2$
W	:	accommodation and recovery variable
t	:	time
a	:	positive constant [0.7]
b	:	positive constant [0.8]
ϕ	:	temperature-scaling factor [0.21]

2.5 Comparison

In the HH, the ML type-II, and the FN models, the relation of the input intensity to the firing time is non-monotone decreasing while that in the IF and the ML type-I models it is monotone decreasing. The parameters, such as the membrane potential, in the HH, IF, and ML models have meaningful dimension, but the parameters in the FN model are not. The characteristics of all the models are summarized in Table 6. The FN model that is simplified from the HH model still remains the relations of the input intensity to the firing time that is the same as the relations for the original HH model despite its qualitativeness. The ML model can show both the non-monotonic and the monotonic relation.

Table 6 Model characteristics.

model	relation of input intensity to firing time	parameters
HH (Hodgkin-Huxley)	non-monotone	quantitative
IF (integrate-and-fire)	monotone	quantitative
ML (Morris-Lecar) type-I	monotone	quantitative
ML (Morris-Lecar) type-II	non-monotone	quantitative
FN (FitzHugh-Nagumo)	non-monotone	qualitative

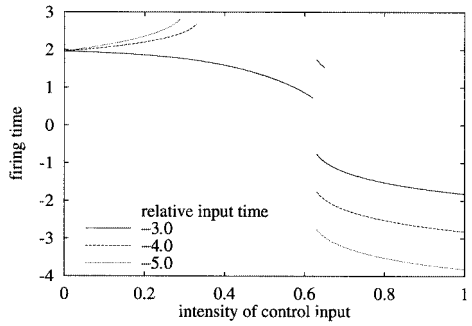

(a)

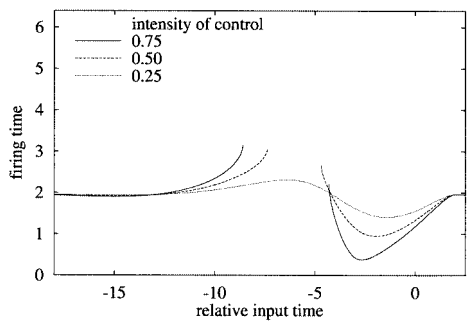

(b)

Fig. 5 Relation of input intensity to firing time by interference in the case of the FitzHugh-Nagumo model. (a) Relation of input intensity to firing time by interference between two inputs. Intensity of base input is 1.0. (b) Relation of relative input time to firing time by interference between two inputs.

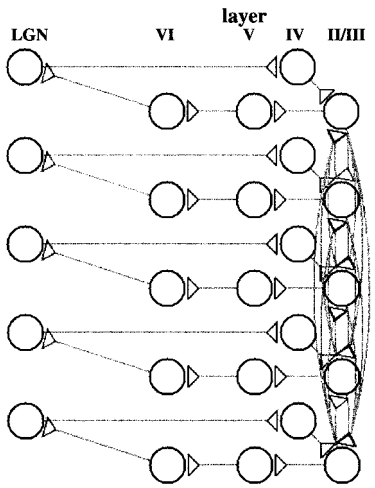

Fig. 6 V1 and LGN model.

3. Firing Patterns in Circular and Mutual Connections

In the previous section, the HH, the ML type-II, and the FN models belong to the group of a non-monotonous relation between the input intensity and the firing time while the IF and the ML type-I models belong to the group of a monotonous one. The firing patterns are supposed to be quite different if the region of weak inputs is used. In this section, we present a connective model of V1 and LGN (lateral geniculate nucleus) to show how different firing patterns depending on model neurons are.

3.1 Model

There is a circular connections in V1 and LGN: from LGN to the layer IV, from layer IV to layer II/III, from layer II/III to layer V, from layer V to layer VI, and from layer VI to the LGN [17], and the neurons of layer II/III of which characters are the same have weak mutual excitatory connections [18]–[20]. We construct a V1 and LGN model with the circular and mutual excitatory connections shown in Fig. 6. This model was designed by our simulation environment [21] and the kernels of the environment (simulation program) of the HH, the IF, the ML and the FN models have been prepared.

The weights of all circular connections are simply set enough to induce a firing of the target neuron; the weights of circular connections are set the base input intensity shown in Sect. 2, which we define as a unit of the weight, in each model. The weights of all mutual excitatory connections are set 0.15 units because the horizontally evoked EPSP (excitatory postsynaptic potential) was too small to elicit spikes [19], [20], [22]. In this model all action potentials propagate after the propagative delay, 0.35 ms (e.g., synaptic delay is 0.29 ms [23] and added the conductive delays).

3.2 Results

First, stimulus is given to five LGN neurons as shown in Fig. 6 in turn from the bottom (the spikes separated constantly; interval = 3.0 ms). The results in the HH, the ML type-II, and the FN model neurons are that the spikes that are scattered at first gradually synchronize as shown in Figs. 7 (a), (d) and (e), respectively. This

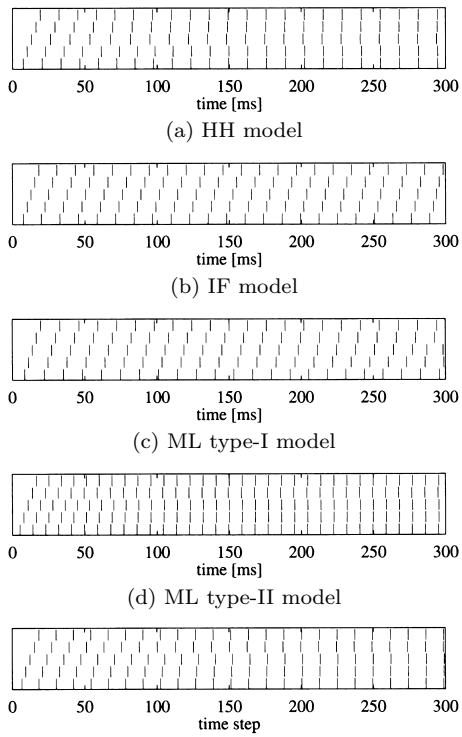

Fig. 7 Comparison firing patterns of five neurons in II/III layer as shown in Fig. 6. Vertical axis indicate the neurons in II/III layer. Vertical bars indicate firings. In each simulation, we use the same model neuron for all V1 and LGN neurons. Though we use the same connective network as shown in Fig. 6, we change a model neuron. Used parameters in each model neuron are the same in Sect. 2 for adjusting the inter spike interval.

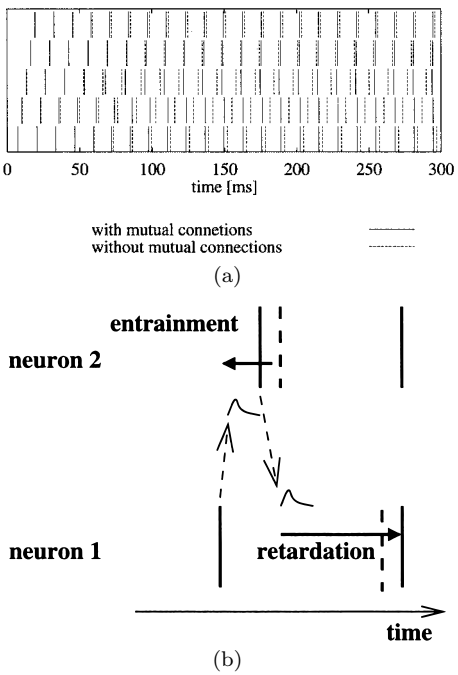

Fig. 8 (a) Effect of mutual connections in case of HH model neuron and (b) Schematic diagram of synchrony by retardation and entrainment of two neurons. Vertical bars indicate firing time. Solid vertical bars are firings with mutual connections while dashed vertical ones are firings without mutual connections. Dashed arrows means propagations of spikes by mutual connections, and in the point of the arrows a weak EPSP (excitatory postsynaptic potential) affects the other neuron. First, the weak EPSP propagates from neuron 1 to neuron 2. In this case, the firing time is advanced because the weak EPSP is near to the strong EPSP from the circular network. Second, the weak EPSP propagates from neuron 2 to neuron 1. In this case, the firing time is retarded because the weak EPSP is far to the strong EPSP from the circular network.

is because the spikes from mutual excitatory synapses retard the distant later spikes from the circular connections and attract the near spikes from the circular connections. This situation can be understood by comparing the result with the mutual connection (solid lines in Fig. 8 (a)) and the result without mutual connection (dashed lines in Fig. 8 (a)). From Fig. 8 (a), a schematic diagram of synchrony by the retardation and the entrainment is shown in Fig. 8 (b). The weak EPSP from the neuron 1 to the neuron 2 in Fig. 8 (b) entrains the near EPSP from the circular network (for example, see the firing time from -3 to 2 ms in Fig. 1 (b)). The weak EPSP from the neuron 2 to the neuron 1 in Fig. 8 (b) retards the later spike because the weak EPSP and the later EPSP from the circular network are apart (for example, see the firing time from -8 to -3 ms in Fig. 1 (b)). In the case of the IF and the ML type-I model neurons, on the other hand, the results were extremely different from the results of the HH and the FN model: the spikes in the case of the IF and the ML type-I model do not synchronize as shown in Figs. 7 (b) and (c), respectively.

We show the firing patterns by stimuli described below in each model neurons. Visual information about the external world is acquired during a fixation period that lasts from 200 to 300 ms and that follows a saccade at by some tens of milliseconds [24]. Psychophysical measurements have indicated that information is actually acquired only during the first roughly 100 ms of the fixation [25]–[29]. We therefore gave five input stimuli (intensity of the base input) to each LGN neuron at random times within the first 100 ms. Each simulation lasts for 300 ms and is repeated 100 times.

The results are shown in Figs. 9, 10, 11, 12, and 13 as the normalized joint peristimulus time histograms (JPSTHs) [30]. The cross-correlations of two layer II/III neurons connected horizontally in the HH (Fig. 9), the ML type-II (Fig. 12), and the FN model (Fig. 13) are high value. The PST coincidence histogram (running from lower left to upper right in the right hand) in Figs. 9, 12, and 13 shows that the spikes gradually elicit coincidence. On the other hand, the cross-correlations of the neurons in the IF (Fig. 10) and the ML type-I model (Fig. 11) are low; the spikes in the IF and the ML type-I model do not synchronize.

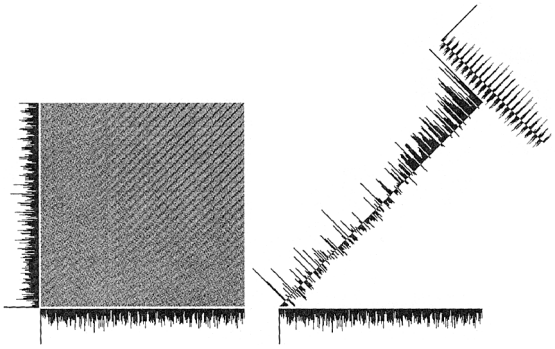

Fig. 9 JPSTH (joint peristimulus time histogram) in case of the Hodgkin-Huxley model. The bottom and the left of the JPSTH along horizontal and vertical axis are peristimulus time histogram (PST) of two neurons. The histogram running from lower left to upper right is PST coincident histogram. The histogram running from upper left to lower right is cross-correlation histogram. Simulation lasted for 300 ms and was repeated 100 times. Bin width is 1.0 ms. Scale bars of PST, coincidence, and cross-correlation histograms are 0.25, 0.8, and 0.16, respectively. Values in a JPSTH matrix are displayed by using gray levels: the higher the value, the darker the gray. The effective connectivity (value of average PST coincidence histogram) is 0.0742. Oscillation frequency is about 75 Hz.

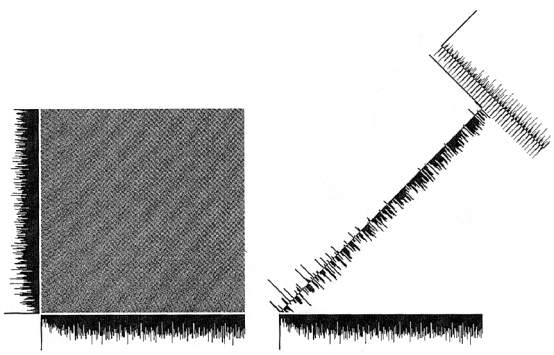

Fig. 10 JPSTH in case of the integrate-and-fire model. The effective connectivity is −0.0684.

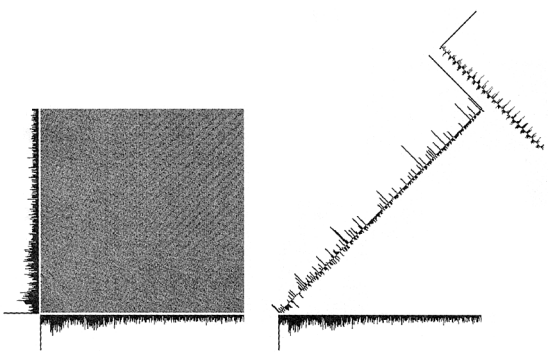

Fig. 11 JPSTH in case of the Morris-Lecar type-I model. The effective connectivity is 0.0015.

4. Discussion

In this paper we show that the firing patterns dramatically change with the dependence on the model neurons. The model characteristics, non-monotone or monotone, as shown in Table 6 are one of the best category to distinguish accurate firing patterns in a connective network model.

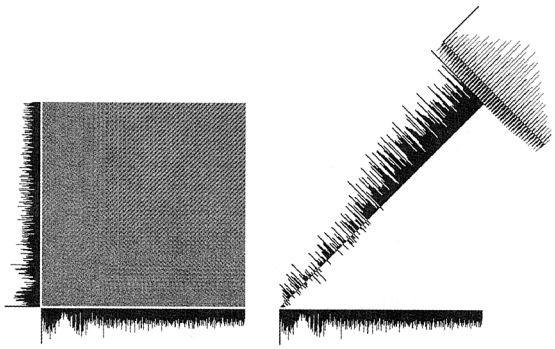

Fig. 12 JPSTH in case of the Morris-Lecar type-II model. The effective connectivity is 0.2393.

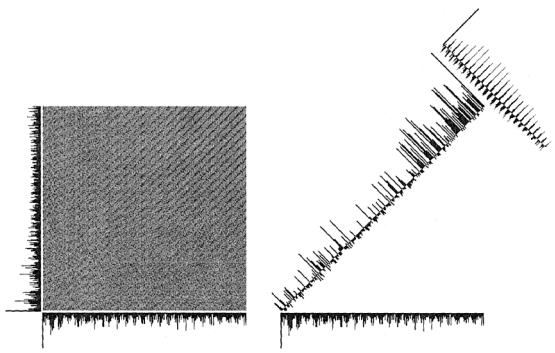

Fig. 13 JPSTH in case of the FitzHugh-Nagumo model. The effective connectivity is 0.0738.

The oscillations of the model described in this article are evoked in the circular connections of area V1 and the LGN. No matter what oscillatory mechanism is, the oscillatory synchronous firing by the interference between spikes in mutual connections can be performed. Examples of another oscillatory mechanisms are the oscillation in a single intrinsically oscillating neurons or in excitatory neuron with recurrent inhibition or in mutual inhibition [31] or in the another loops. Gastelo-Branco et al. [32] made simultaneous multi-unit recordings from visual areas 17 (V1) and 18 as well as the LGN in order to examine the interactions between subcortical and cortical synchronization mechanisms. Strong correlations of oscillatory responses were observed. In the static stimuli the oscillation frequencies of both cortical neurons and LGN neurons were 60–120 Hz, in agreement with our simulation results, while in the dynamic stimuli the oscillation frequencies of cortical neurons and LGN neurons were different: the frequencies of cortical neurons were 20–60 Hz while the frequencies of LGN neurons were 60–120 Hz. In the latter one, we suppose that multiple loops affect the

oscillations.

It is a future work to examine firing time by interference between spikes in more neural connective models. We would like to further examine the firing time in neural circuits in order to clarify the coding mechanism which utilizes the spike timing in the nervous system.

Acknowledgments

This work was supported in part by Research for the Future Program of Japan Society for the Promotion of Science, by a Grant-in-Aid for Scientific Research on Priority Areas (No.10164215) from the Ministry of Education Science, Sports and Culture of Japan, by the Kayamori Foundation of Informational Science Advancement, and by the Tateisi Science and Technology Foundation.

References

[1] Z.F. Mainen and T.J. Sejnowski, "Reliability of spike timing in neocortical neurons," Science, vol.268, pp.1503–1506, 1995.
[2] C. Koch, "Computation and the single neuron," Nature, vol.385, pp.207–210, 1997.
[3] A.L. Hodgkin, "The local electric changes associated with repetitive action in a non-medullated axon," J. Physiol. (Lond.), vol.107, pp.165–181, 1948.
[4] K.S. Cole, Membranes, Ions and Impulses, University of California Press, Berkeley and Los Angeles, California, 1968.
[5] K. Murakoshi and K. Nakamura, "A neural mechanism of adjusting timing of spikes by intensity of input for dynamic coding," Soc. Neurosci. Abstr., vol.24, no.655.12, p.1672, Los Angeles, California, 1998.
[6] K. Murakoshi and K. Nakamura, "Analysis of change in spike timing with interference between synaptic inputs," IEICE Trans., vol.J82-D-II, no.12, pp.2385–2393, Dec. 1999.
[7] A.L. Hodgkin and A.F. Huxley, "A quantitative description of membrane current and its application to conduction and excitation in nerve," J. Physiol. (Lond.), vol.117, pp.500–544, 1952.
[8] A. Zador, C. Koch, and B.T. H., "Biophysical model of a Hebbian synapse," Proc. Natl. Acad. Sci. USA, vol.87, pp.6718–6722, 1990.
[9] Ö. Bernander, R.J. Douglas, K.A.C. Martin, and C. Koch, "Synaptic background activity influences spatiotemporal integration in single pyramidal cells," Proc. Natl. Acad. Sci. USA, vol.88, pp.11569–11573, 1991.
[10] M.A. Arbib, ed., The Handbook of Brain Theory and Neural Networks, MIT Press, Cambridge, Massachusetts, 1995.
[11] C. Morris and H. Lecar, "Voltage oscillations in the barnacle giant muscle fiber," Biophys. J., vol.35, pp.193–213, 1981.
[12] J. Rinzel and B. Ermentrout, "Analysis of neural excitability and oscillations," in Methods in neuronal modeling: from synapses to networks, Computational Neuroscience, chapter 5, eds. C. Koch and I. Segev, pp.135–169, MIT Press, 1989.
[13] B.S. Gutkin and G.B. Ermentrout, "Dynamics of membrane excitability determine interspike interval variability: A link between spike generation mechanisms and cortical spike train statistics," Neural Computation, vol.10, pp.1047–1065, 1998.
[14] R. FitzHugh, "Impulses and physiological states in theoretical models of nerve membrane," Biophys. J., vol.1, pp.445–466, 1961.
[15] R. FitzHugh, "Mathematical models of excitation and propagation in nerve," in Biological Engineering, vol.9 of Inter-University Electronics Series, chapter 1, ed. H.P. Schwan, pp.1–85, McGraw Hill, New York, 1969.
[16] J. Nagumo, S. Arimoto, and S. Yoshizawa, "An active pulse transmission line simulating nerve axon," Proc. IRE, vol.50, pp.2061–2070, 1962.
[17] C.D. Gilbert, "Microcircuitry of the visual cortex," Ann. Rev. Neurosci., vol.6, pp.217–247, 1983.
[18] C.D. Gilbert, "Horizontal integration and cortical dynamics," Neuron, vol.9, pp.1–13, 1992.
[19] A. Mason, A. Nicoll, and K. Stratford, "Synaptic transmission between individual pyramidal neurons of the rat visual cortex *in vitro*," J. Neurosci., vol.11, pp.72–84, 1991.
[20] J.A. Hirsch and C.D. Gilbert, "Synaptic physiology of horizontal connections in the cat's visual cortex," J. Neurosci., vol.11, pp.1800–1809, 1991.
[21] K. Murakoshi and T. Kurata, "A simulation environment for designing and examining biological neural network models," IEICE Trans. Inf. & Syst., vol.E79-D, no.8, pp.1212–1216, Aug. 1996.
[22] A.M. Thomson, D. Girdlestone, and D.C. West, "Voltage-dependent currents prolong single-axon postsynaptic potentials in layer III pyramidal neurons in rat neocortical slices," J. Neurophysiol., vol.60, pp.1896–1907, 1988.
[23] C. Wang, B.G. Cleland, and W. Burke, "Synaptic delay in the lateral geniculate nucleus of the cat," Brain Res., vol.343, pp.236–245, 1985.
[24] F.W. Campbell and R.H. Wurtz, "Saccadic omission: Why we do not see a grey-out during a saccadic eye movement," Vision Research, vol.18, pp.1297–1303, 1978.
[25] G.R. Loftus, "Eye fixations and recognition memory for pictures," Cognit. Psychol., vol.3, pp.525–551, 1972.
[26] M.C. Potter and E.I. Leby, "Recognition memory for a rapid sequence of pictures," J. Exp. Psychol., vol.81, pp.10–15, 1969.
[27] I. Biederman, J.C. Rabinowitz, A.L. Glass, and E.W. Stacv, Jr., "On the information extracted from a glance at a scene," J. Exp. Psychol., vol.103, pp.597–600, 1973.
[28] M.C. Potter, "Short-term conceptual memory for pictures," J. Exp. Psychol.: Hum. Learn. and Mem., vol.2, pp.509–522, 1976.
[29] T. Inui and K. Miyamoto, "The time needed to judge the order of a meaningful string of pictures," J. Exp. Psychol.: Hum. Learn. and Mem., vol.7, pp.393–396, 1981.
[30] A.M. Aertsen, G.L. Gerstein, M.K. Habib, and G. Palm, "Dynamics of neuronal firing correlation: Modulation of "effective connectivity"," J. Neurophysiol., vol.61, pp.900–917, 1989.
[31] R. Ritz and T.J. Sejnowski, "Synchronous oscillatory activity in sensory systems: New vistas on mechanisms," Curr. Opin. Neurobiol., vol.7, pp.536–546, 1997.
[32] M. Castelo-Branco, S. Neuenschwander, and W. Singer, "Synchronization of visual responses between the cortex, lateral geniculate nucleus, and retina in the anesthetized cat," J. Neurosci., vol.18, pp.6395–6410, 1998.

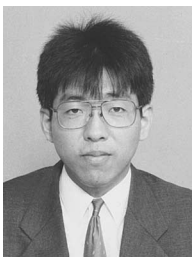

Kazushi Murakoshi was born in Chiba, Japan, in 1968. He received the B.Eng., M.Eng. and Dr. Eng. degrees in Electronics Engineering from Chiba University, Japan in 1991, 1993, and 1997, respectively. Since 1997, he has been a research associate in Department of Computational Intelligence and Systems Science, Interdisciplinary Graduate School of Science and Engineering, Tokyo Institute of Technology. His interests include biological neural network mechanisms. He is a member of JNNS, JCSS, Vision Society of Japan, Japan Neuroscience Society and Society for Neuroscience.

Kiyohiko Nakamura was born in Osaka, Japan, in 1953. He received the B.S., M.S., and Ph.D. degrees in mechanical engineering from Kyoto University, Kyoto, Japan, in 1977, 1979, and 1983, respectively. He is currently a professor in Department of Computational Intelligence and Systems Science, Interdisciplinary Graduate School of Science and Engineering, Tokyo Institute of Technology. His research interests are in systems and computational neurosciences, especially neural mechanisms of imagery processing. He is a member of JNNS, SICE, ISCIE, Japan Neuroscience Society and Society for Neuroscience.